Available online at www.sciencedirect.com
ScienceDirect
Journal of the European Ceramic Society 27 (2007) 2541–2547
www.elsevier.com/locate/jeurceramsoc

Rapid formation of α-sialon during spark plasma sintering: Its origin and implications

David Salamon [a], Zhijian Shen [a,*], Pavol Šajgalík [b]

[a] *Department of Inorganic Chemistry, Arrhenius Laboratory, University of Stockholm, S-106 91 Stockholm, Sweden*
[b] *Institute of Inorganic Chemistry, Slovak Academy of Sciences, SK-845 36 Bratislava, Slovakia*

Received 24 June 2006; received in revised form 11 September 2006; accepted 16 September 2006
Available online 27 October 2006

Abstract

α-Sialons with varied chemical compositions and starting precursors were sintered in spark plasma sintering (SPS) furnace to verify the influence of electrical conduction, mechanical pressure and heat transfer efficiency. The internal temperature that the sample was exposed to and its evolution during the heating were experimentally estimated and discussed. XRD and SEM grain size analysis were carried out to evaluate the phase and microstructure evolution. Mechanical pressure was eliminated to create a free sintering condition under SPS. By free sintering and surrounding the sample with graphite wool the heat transfer was sufficiently retarded and a usual slow reaction was demonstrated. It is verified that the efficiency of heat transfer is more influential in the enhancement of α-sialon formation and grain growth by SPS than the efficiency of electric conduction.

Keywords: SPS; Sialon; Microstructure

1. Introduction

Spark plasma sintering (SPS), also named plasma activated sintering,[1] is a method applicable for the sintering of metals and ceramics, consolidation of polymers, joining of metals, and for enhancing crystal growth and chemical reactions. In general, the method is very similar to conventional hot-pressing, but instead of using an external heating source, a pulsed direct current is passed through the electrically conducting pressure die and, in appropriate cases, also through the sample, implying very efficient heating. The unique features of this process are the possibilities to apply very fast heating rates, several hundred degrees per minute, and to achieve full densification within minutes. The origin of such a radical enhancement of densification is still under debate. In the literature, the influence of the electrical field and/or pulsed dc on the densification and grain growth has been investigated,[2,3] whereas the generation of plasma has not been experimentally confirmed yet (especially when non-conductive ceramic powders were compacted).

For sintering of Si_3N_4-based ceramics, the pulsed electric current and field was suggested to promote mass transfer and diffusion of charged species in the liquid phase,[4] and the applied higher-than-normal pressure was believed to enhance viscous flow thus promoting densification.[4] In the case of α-sialons the formation of α-sialon and other phases by reaction of the precursor reactants, α-Si_3N_4/β-Si_3N_4, AlN and R_2O_3 (R labeling a rare-earth element) is very rapid, and thus they are very sensitive to the densification conditions of the final body. It has been well established that these reactions take place via a solution-reprecipitation mechanism, implying that the dissolution of the reactants and the oversaturation of α-sialon were enhanced by the SPS process.[5]

The present work aimed to explore the origin and implications of such enhancements by spark plasma sintering using the formation of α-sialon as an indicator. Accordingly, we have investigated the influence of three critical parameters on the formation of α-sialon: the mechanical pressure, the electrical current and the thermal conductivity between the graphite die and the sample. The commonly concerned temperature issue was also addressed. The sintering of selected sample using conventional hot-press (HP) and gas pressure sintering (GPS) was carried out to produce reference samples for comparison. The

* Corresponding author. Tel.: +46 816 2388; fax: +46 815 2184.
E-mail address: shen@inorg.su.se (Z. Shen).

0955-2219/$ – see front matter © 2006 Elsevier Ltd. All rights reserved.
doi:10.1016/j.jeurceramsoc.2006.09.008

role of the phase composition of starting mixtures for the formation of α-sialons was also shortly discussed.

2. Experimental

The precursor powders used in this study are α-Si_3N_4 (UBE-SN-E10, containing 1.5 wt.% O), β-Si_3N_4 (Denka SN-F1, containing less than 10% α-Si_3N_4 and ~2.0% O, $d_{50} = 3\,\mu m$), AlN (HC Starck Grade C, containing 1.6 wt.% O), Y_2O_3 (Alfa Aesar 99.99%), and Yb_2O_3(PiCD 99.95%). Five batches with four different overall chemical compositions were investigated. They were labelled as ARXXXX or BRXXXX, with R representing the rare-earth used for doping (either Y or Yb), A and B representing the α- and β-Si_3N_4 powder in the starting batch, respectively, the four digits XXXX representing the x- and n-values in the general formula of α-sialon, $RE_xSi_{12-(3x+n)}Al_{3x+n}O_nN_{16-n}$, with the two first digits equals 100 times x and the last two equals 10 times n. Thus, AY3510 means a α-Si_3N_4-based Y-sialon with the x and n-values equal 0.35 and 1.0, respectively. In calculating the aimed compositions the amounts of oxygen impurity in Si_3N_4 and AlN powders were taken into account. All starting powders were ball-milled in isopropanol with Si_3N_4 balls for 24 h. The mixed powders were then dried and pressed into cylinders under a uniaxial pressure of 100 MPa, followed by cold isostatic pressing at 250 MPa. In case of SPS processing under mechanical pressure the dried powders were poured into the graphite die directly and pre-pressed uniaxially at pressure below 100 MPa.

The SPS processing was carried out in vacuum in an SPS apparatus, Dr. Sinter 2050 (Sumitomo Coal Mining Co. Ltd., Japan). The temperature was automatically raised to 600 °C over a period of 3 min, and from this point and onwards it was monitored and regulated by an optical pyrometer focused on the surface of the die. The heating rates of 100 °C min^{-1} and (in certain cases) 20 °C min^{-1} were used. Unless specified otherwise a uniaxal pressure of 50 MPa was applied over the duration of the sintering cycle. This set-up allows a cooling rate of ~400 °C min^{-1} in the temperature range 1800–1000 °C. The graphite die was made by assembling a cylinder, two punches and (in certain cases) an inserted ring made the graphite die. The dimensions of the graphite components are as follows: (1) graphite cylinder: inner diameter = 15 mm, outer diameter = 35 mm, height = 30 mm; (2) graphite punches: height = 15 mm; (3) graphite ring: inner diameter = 13 mm, outer diameter = 15 mm, height = 10 mm. A pulse pattern of 12:2 (12 pulses on and 2 off) was used in all cases.

The samples, either as the starting powder mixture of compacted green bodies, were loaded into the die in one of the following manners, see also Fig. 1:

(1) A conductive graphite sheet was used to separate the sample from the die and punches, and a uniaxial pressure is used.
(2) The green body is embedded in BN powder, i.e. the sample is an electrically insulated from the punches and cylinder. BN powder matrix is more than 1 mm thick. The processing is done under a uniaxial pressure.

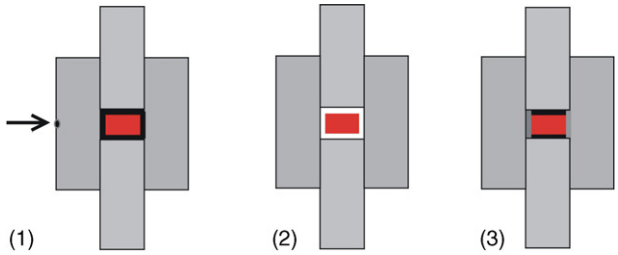

Fig. 1. Schematic drawing of sample encasing during the experiments. (1) The traditional encasing with the conductive graphite paper for sample separation. (2) The sample separated by h-BN powder. (3) The sample separated by a graphite ring and graphite paper. The arrow shows the position of the focused pyrometer.

(3) Pressure-less sintering, i.e. by inserting a graphite ring with height larger than the compacted green bodies to avoid any possible mechanical pressure on the sample. Mechanical pressure of punches on the graphite ring results in high current density inside the ring and higher temperature (see below). The other effect of pressure on the ring is that it closes the system inside the ring from the outside atmosphere. The sample was separated from the graphite punches on both sides by either graphite paper or graphite paper and graphite wool, yielding two more thermal and electric conducting patterns.

The hot-pressing (HP) was done at 1700 °C with a dwell time of 1 h and mechanical pressure of 30 MPa. Gas pressure sintering of the AY4011 composition was carried out at 1750 °C with a dwell time of 2 h under 3 MPa of nitrogen. Table 1 summarizes the processing conditions. If not otherwise specified, the temperatures mentioned below always refer to the ones directly measured by pyrometer focused on the outside wall of the graphite die.

Grain size analysis was done on SEM pictures of fracture surface. A minimum of 2000 grains were characterized for each measured sample. The reported values are in μm^2, which describe grain size distribution in two-dimensional SEM pictures. Phase compositions were determined by powder XRD using a Guinier–Hägg camera with Cu Kα1 radiation and Si as an internal standard. Pressure-less sintered sample were also measured also without Si addition, to verify the possible formation of free Si during the process. The unit cell parameters were refined with PIRUM computer software,[6] and the obtained cell parameters are summarized in Table 2.

The real temperatures that the samples were exposed to inside the graphite dies were verified by imbedding into the dies wires of the pure gold, silver or platinum, and comparing the measured temperatures at which they melt to their literature values (Ag = 962 °C, Au = 1064 °C, Pt = 1768 °C). The chipped wires from the pure metal were placed into sockets in a pellet then covered with another thin pellet made of a BN-Si_3N_4 composite pre-sintered at 1800 °C. An additional thin layer of BN powder was used on the top and bottom sides of the sintered pellet to spread mechanical pressure. After sintering over the metal's melting temperature, the chipped wires become shining balls. In some cases just surface melting is observed and the formation of a neck between two parts of wire was seen under optical micro-

Table 1
Description of experiment conditions and the samples final density

Name	Composition	Protection	Maximum temperature (°C)	Temperature rate (°C min^{-1})	Dwell (min)	Press (MPa)	Density (g cm^{-3})	Phase assemblage
AY3510-BN	AY3510	BN	1700	100	3	50	3.19	α′(s)
AY3510-C	AY3510	Graphite	1700	100	3	50	3.22	α′(s)
AY3510-Ring	AY3510	Ring	1700	100	3	0	3.06	α′(s), SiC (vw)
AY4011-BN	AY4011	BN	1700	100	3	50	3.28	α′(s)
AY4011-C	AY4011	Graphite	1700	100	3	50	3.22	α′(s)
AY4011-Ring	AY4011	Ring	1700	100	3	0	3.02	α′(s), SiC (vw)
AY5013-BN	AY5013	BN	1700	100	3	50	3.28	α′(s)
AY5013-C	AY5013	Graphite	1700	100	3	50	3.16	α′(s)
AY5013-Ring	AY5013	Ring	1700	100	3	0	2.89	α′(s), SiC (vw)
AYb4211-20 C	AYb4211	Graphite	1600	20	5	50	3.49	α′(s), α (vw)
AYb4211-C	AYb4211	Graphite	1600	100	5	50	3.49	α′(s), α (vw)
AYb4211-Ring	AYb4211	Ring	1600	100	5	0	2.65	α′(s), α (vw)
AYb4211-Ring + W	AYb4211	Ring + wool	1600	100	5	0	–	α′(s), α (vw), β′ (w), $Yb_2Si_2O_7$ (vw)
BYb4212-20 C	BYb4212	Graphite	1600	20	5	50	3.21	α′(s), β (w), $SiAl_6O_2N_6$ (vw)
BYb4212-C	BYb4212	Graphite	1600	100	5	50	3.23	α′(s), β (s), $SiAl_6O_2N_6$ (vw)
AY4011-HP	AY4011	BN	1700	10	60	30	3.23	α′(s)
AY5013-HP	AY5013	BN	1700	10	60	30	3.26	α′(s)
AY4011-GPS	AY4011	Crucible	1750	7	120	3 of N_2	–	α′(s), $Y_2Si_3O_3N_7$ (vw)

Remarks: α′, α-sialon; β′, β-sialon; α, α-Si_3N_4; β, β-Si_3N_4; s, strong; w, weak; vw, very weak.

scope. Such cases were attributed to an overshoot influence and were observed only when the heating rate 100 °C min^{-1} was applied. Decreasing the heating rate to 20 °C min^{-1} minimums 100 °C before final temperature diminished the overshoot. Using the heating rate 20 °C min^{-1} greatly reduces this overshoot. Another way of determining the overshoot is the calculation of the delay of heat transfer between the hottest part (punches) and measured part (cylindrical die). The calculation of the temperature can be done when current is linearly proportional to the temperature. This presumption is correct as long as heat loss does not play an important role. A linear correlation is obvious for the relatively small graphite dies, with high heating rates and temperatures over 800 °C. The time difference between the maximal measured temperature and maximal current under these conditions is a constant value for each particular sets up. This calculated time is then the transfer delay. Multiplying this transfer delay time by the heating rate gives the temperature overshoot.

Table 2
Unit cell parameters of selected Y-sialons and Yb-sialons

Name	a (Å)	c (Å)	V (Å^3)
AY3510-BN	7.8085(4)	5.6882(6)	300.36
AY3510-C	7.8099(4)	5.6863(5)	300.37
AY3510-Ring	7.8108(2)	5.6882(2)	300.56
AY4011-BN	7.8164(2)	5.6951(3)	301.33
AY4011-C	7.8163(3)	5.6939(4)	301.26
AY4011-Ring	7.8172(1)	5.6949(2)	301.39
AY5013-BN	7.8272(1)	5.7050(2)	302.71
AY5013-C	7.8291(5)	5.7027(6)	302.72
AY5013-Ring	7.8248(5)	5.7029(8)	302.39
AYb4211-20 C	7.8204(2)	5.6993(2)	301.88
AYb4211-C	7.8212(2)	5.7005(3)	301.99
AYb4211-Ring	7.8209(4)	5.6984(4)	301.86
AYb4211-Ring + W	7.8183(6)	5.6949(6)	301.46
BYb4212-20C	7.8197(3)	5.6968(3)	301.68
BYb4212-C	7.8361(5)	5.7126(5)	303.78

3. Results and discussions

Prior to dealing with the main aim of this paper the experiments leading to the determination of the true sample temperature were performed. This is extremely important with respect to the controlling the phases and microstructure for the obtained α-sialons.

3.1. The temperature

Calculations from the literature and our own experiences[7] revealed that the hottest parts in graphite tooling set are the up and lower punches. Good connection between graphite die and punches (insured by mechanical pressure) increase the electric current going through the die. Heat transfer delay results in a temperature overshoot. Fig. 2 presents temperature and current profiles.

3.1.1. The overshoot

The calculation of the time difference presenting between the achieved maximal current and achieved maximal temperature revealed a time delay of 24 ± 6 s (the measured transfer delay is constant, for all of our experiments in which heating rate 100 °C min^{-1} was used). When a heating rate of 100 °C min^{-1} is used, this time delay implies a temperature overshoot of approximately 50 °C. This calculation is in good agreement with the direct experimental observation of the partial melting of pure metals. The overshoot is strongly connected with heating rate.

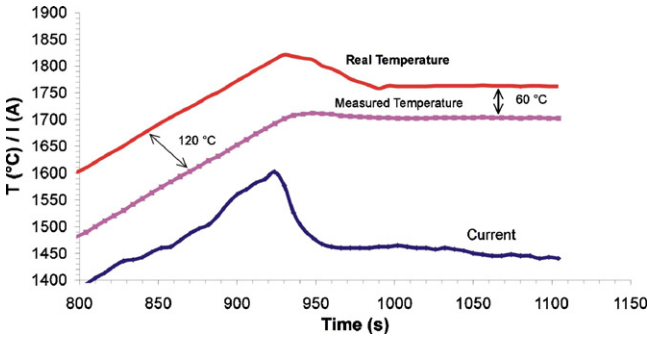

Fig. 2. Temperatures and current developments during SPS.

Both the maximal temperature achieved and the time that the sample was exposed to it are important for the phase evolution. They may accelerate mass transfer processes as phase formation and crystallization, as will be discussed below.

3.1.2. The real temperature during the dwell time

The estimated real temperatures in each experimental set-up are summarized in Table 3. The temperature variations are not very big during the dwell time, but the temperature overshoot accompanying with the high heating rate increases this temperature variation. In general, when mechanical pressure is used, the real temperature that the sample is exposed to after the initial overshoot is $60 \pm 20\,^{\circ}C$ higher than the set one. This temperature difference increases to $80 \pm 20\,^{\circ}C$ when a graphite ring is inserted into the die to remove the mechanical pressure. Although the overshoot last just a few seconds, a significant excess of heat transfer to the sample during this short time, as verified by the partially melted surface of gold wires. Samples sintered under mechanical pressure are about 1–2 mm in height and only about 20% of its surface is in contact with the relatively cold cylinder part, the rest of the surface being in contact with the hotter punch surfaces. If the heat transfer to the cylinder (measured part) takes at maximum 30 s and counting the thickness of cylinder as 10 mm, then heat transfer to the sample (and temperature homogenization) should be more than possible. Under hot-pressing, a temperature gradient between punches and cylinder is also present, but it is very small (in our case around 10 °C), because, the distance between the sample and heating element is not more than 10 mm, of which 2 mm is "field" with nitrogen gas and the rest is graphite. The time needed to transfer heat to the sample will be longer in HP than in the case of SPS, but further investigation and calculation is necessary for the evaluation of such differences. The GPS samples have the slowest heat transfer from the heating elements to the samples. In this case, the heat transfer distance is approximately 50 mm that composes two zones filled with, respectively, gas (nitrogen) and solid (crucible).

3.2. The electrical conductive connection between the die and sample

Under pressure no differences between conductive connected and non-conductive connected samples was observed. In all cases phase analysis revealed the presence of only pure α-sialon. There were no significant differences among the compositions with different x-values ($x = 0.35$, 0.40, 0.50). In both conditions the α-sialon formation was completed and no other phases were detected by XRD after sintering at 1700 °C for 3 min, see Fig. 3. The grain size analysis showed no significant difference in microstructure between the conductively connected and non-connected samples. The main differences in grain size distribution are between the different compositions, as revealed in Fig. 4. The unit cell parameters are very similar for the same starting compositions and different conditions; the unit cell volume increases with the x-value.

Adding a separating layer of h-BN between the sample and punches breaks the current passing through the samples, but may have very limited influence on heat transfer between the punches and the sample. Such a heat transfer is more determined by the thermal conductivity of the processing samples. Low thermal conductivity of the sample promotes faster heat transfer from the punches (hot part) to the cylinder (measured part) rather than to the sample. It should be pointed out as well, that the heat transfer is encouraged by mechanical pressure in the direction from the punch towards the samples.

3.3. The mechanical pressure

SPS is known as a pressure-assisted process. When the sample is loaded in "free sintering" condition, the benefits added by mechanical pressure are totally removed. Under this condition, a small amount of SiC grains not so homogeneously distributed all over the sample and on the graphite wall was formed besides the aimed α-sialon phase in sintered AY-sialon compositions. However, free silicon possibly forming by the decomposition of Si_3N_4 was not detected, see Fig. 5. AYb-sialon compositions free sintered at 1600 °C showed also the forma-

Table 3
Temperature evaluation of real temperature behaviour in the SPS system compared to measured temperatures

Conditions	Measured by pyrometer (°C) (mentioned in text)	Maximal touched temperature during the overshoot (°C)	Maximal time of overshoot (s)	Dwell temperature after stabilization (°C)
Graphite separation, 50 MPa, 100 °C min^{-1}	1700	1800–1840	30	1740–1780
BN separation, 50 MPa, 100 °C min^{-1}	1700	1800–1840	30	1740–1780
Graphite ring, 0 MPa, 100 °C min^{-1}	1700	1820–1860	30	1760–1800
Graphite separation, 50 MPa, 20 °C min^{-1}	1600	1660–1700	30	1640–1680
Graphite separation, 50 MPa, 100 °C min^{-1}	1600	1700–1740	30	1640–1680

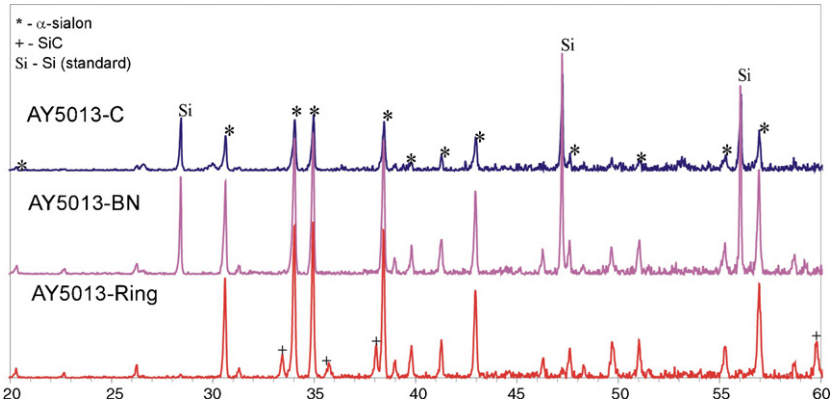

Fig. 3. XRD diffraction pattern of a AY5013 sample sintered at 1700 °C.

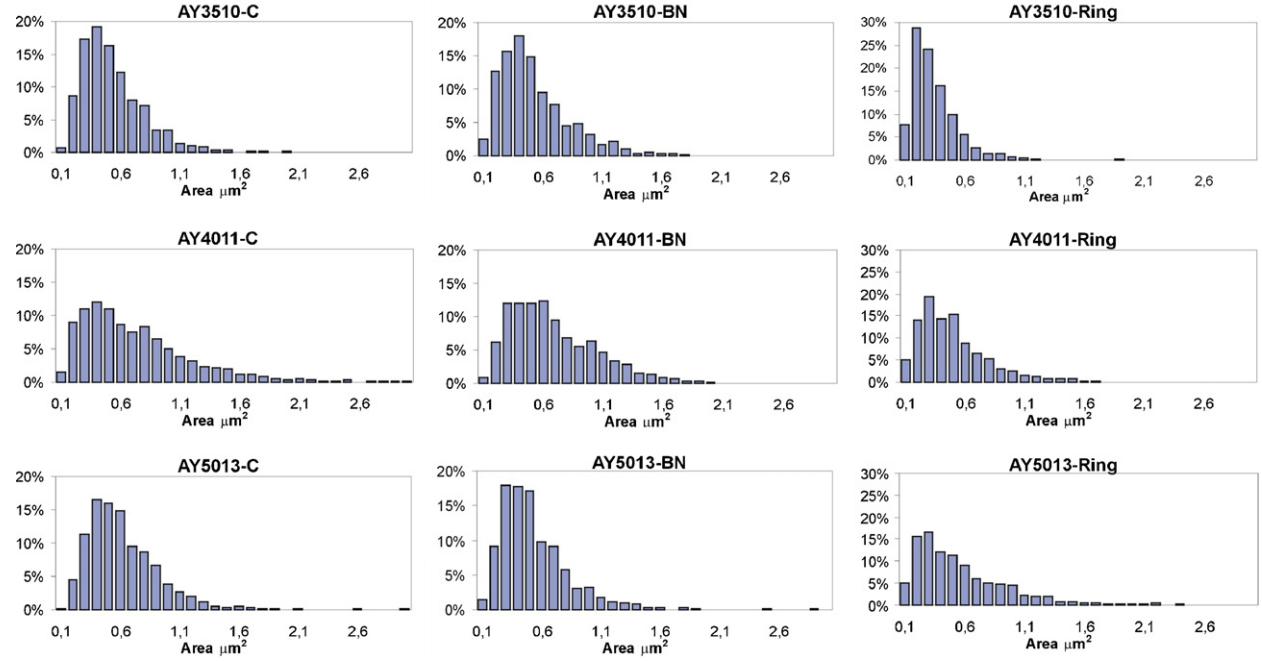

Fig. 4. Grain size distribution of conductive connected samples (C), non-conductive connected samples (BN) and samples sintered without mechanical pressure (Ring).

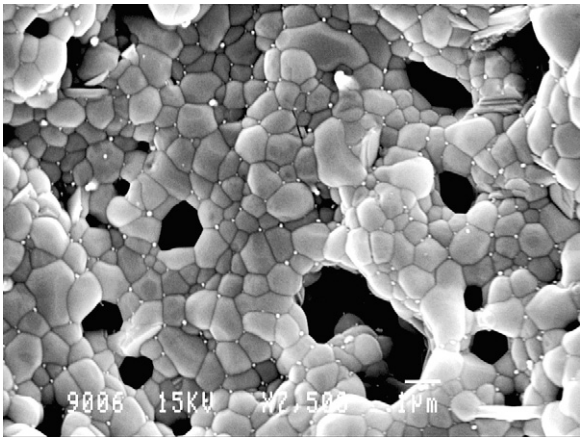

Fig. 5. SEM picture of the sample AY5013-Ring. The very small grains are SiC grains.

tion of SiC, in addition of the weak formation of β-Si_3N_4, see Fig. 6. It should be noticed that the weak formation of β-Si_3N_4 is there in normal SPSed (under mechanical pressure) samples, indicating that its formation not necessarily related to pressure. Under the applied SPS free sintering condition the formation of α-sialon is completed before the complete densification, demonstrating enhanced reaction feature of SPS without additional pressure.

Grain size analysis reveals significant structural differences between samples prepared with and without the application of mechanical pressure, besides the general dependence of grain size distributions on overall chemical compositions, see Fig. 4. These differences may have some connection with small temperature differences (see Table 3), but are mainly the result of mass transfer inside the samples. The SPS free sintered sample with relatively low content of liquid phase (AY3510-Ring) has smaller grains, and the difference between using mechanical

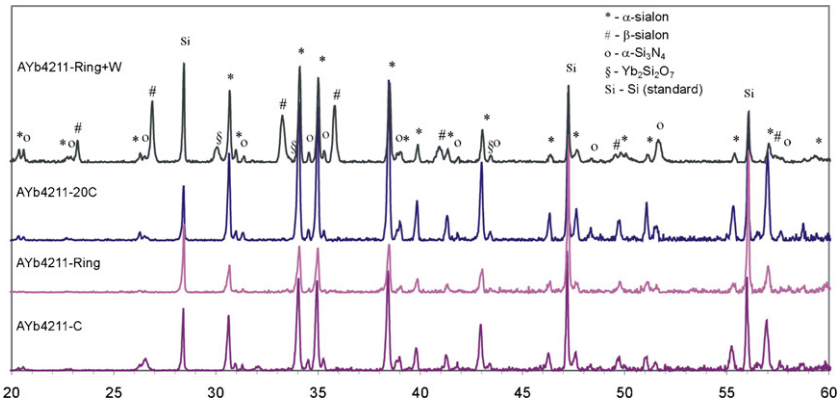

Fig. 6. XRD patterns of AYb4211 sialon at 1600 °C sintered with a dwell time of 5 min. Ring + W—sample sintered without pressure and separated by graphite wool, 20C—sample heated up 20 °C min^{-1}, Ring—sample sintered without pressure, and C—sample sintered under 50 MPa of mechanical pressure.

pressure and free sintering is the most significant. The grain size morphology of free sintered samples is different, and the sintered grains are more rounded, see Fig. 5. The unit cell parameters are not significantly affected by mechanical pressure (Table 2).

The free sintering experiments clearly demonstrate that the mechanical pressure is not necessary for the rapid formation of α-sialons. The shape and density of the SPS free sintered samples are comparable with that of GPSed samples. No significant microstructure deviations inside the SPS free sintered samples have been observed, i.e. they are quite homogeneous in phase composition and microstructure. After SPS free sintering the sample maintains a distance of 1–2 mm towards the graphite ring and the graphite paper (from the upper side), implying that the sample has no direct contact with the heating source in all directions (the sintering shrinkage of sample is around 40%). The observation of the formation SiC crystals on the graphite surface indicates that gases, e.g. CO and SiO, are formed during the sintering, so the sample cavity surrounded by the graphite ring and the punches must be sealed tightly. The absence of silicon indicates that during the sintering α-sialon formation is faster than the decomposition of Si_3N_4 and/or any formed free silicon immediately reacts with carbon source(s) to form SiC. The bulk distribution of nano-SiC grains in the α-sialon-matrix must also imply a gas phase, most probably CO, is involved in the reaction. The loss of silica by the formation of gaseous SiO in the system is probably the reason for the density decrease (Table 1). The formation of this gas is dependent on the temperature and the volume of the cavity around the sample. The same temperature regime promotes the same amount of gas, but the amount of residual SiO_2 available for liquid formation is dependent on the starting composition. Small amount of residual SiO_2 yields the density decrease. A higher amount of Y_2O_3 (higher *x*-value) alone does not help densification.

The α-sialon formation is completed in the GPS (1750 °C for 2 h) sintered sample, AY4011-GPS. XRD analysis showed the presence of a very weak $Y_2Si_3O_3N_4$ phase in addition to α-sialon. The formation of $Y_2Si_3O_3N_4$ phase can be ascribed to the slow heating and cooling rate applied, leading to the partial crystallization of the grain boundary glassy phase.[8]

3.4. The thermal conductive connection between the die and the sample

When graphite wool is used to surround the sample in the cavity under the SPS free sintering condition, the heat transfer between the graphite heating source and the sample is effectively reduced. Doing so, the XRD phase analysis reveals the presence of, besides α-sialon as a major phase, a high content of β-sialon, unreacted α-Si_3N_4, and a oxide phase, $Yb_2Si_2O_7$, see Fig. 6. So far, it has been recognized as one of the unique features of SPS to rapidly form sialon phases while avoiding the formation of any intermediate phases.[9] The observation of the formation of $Yb_2Si_2O_7$ phase clearly demonstrates that without sufficient heat transfer the α-sialon formation would not be enhanced and the formation of low temperature phase, as it is always observed in conventional processes,[10] would be hard to avoid.

The heat transfer from the graphite heating sources to the sample is essential for the formation of α-sialon. Obtaining the same phase structure as SPS by hot-pressing requires a 20 times longer holding time, i.e. 60 min by HP versus 3 min by SPS. Besides the momentarily slightly higher temperature (1740–1780 °C), the impact of an overshoot on enhancing the heat transfer to the sample should not be underestimated. Such an influence is more obvious when the sample contains a relatively low content of liquid phase, e.g. AY3510.

The graphite wool separation also enables us to distinguish the influence of the heating rate and heat transfer efficiency. The heat transfer efficiency is determined by the temperature gradient and thermal conductivity. The impact of high heating rate during SPS is well recognized but not the efficient heat transfer due to the direct contacting of the samples and heating source. Owing to the higher heat transfer efficiency the formation of low temperature phase(s) during reactive sintering of sialon ceramics by SPS is often avoided even when lower heating rates are applied. When the graphite wool is inserted during SPS free sintering the heat transfer efficiency is sufficiently reduced, eliminating the obvious overshoot influence and yielding lower real temperature when short holding times are used. On the other hand, the SPS free sintering conditions are comparable with that of GPS.

3.5. The role of precursors

The sample BYb4212 containing mainly β-Si_3N_4 in the starting mixture forms after SPS α-sialon and contains also high amounts of β-Si_3N_4 and the 21R-polytype ($SiAl_6O_2N_6$). α-Sialon is formed locally and other phases can be easily recognized by their different morphologies. The composition containing mainly α-Si_3N_4 (AYb4211) forms α-sialon in whole volume uniformly and contains a small amount of residual α-Si_3N_4. Previous studies demonstrated that the formation of α-sialon from β-Si_3N_4 proceeds slower than from α-Si_3N_4, because β-Si_3N_4 is more stable than α-Si_3N_4, thus providing a lower driving force.[11] On the other hand, the amount of liquid phase and grain growth is determined mainly by the starting composition, which is an obvious observation also for conventional sintering.[12] The β-Si_3N_4 powder has also coarse grains that may also slow down the process of solution. The α/β-Si_3N_4 ratio in starting mixture also has a strong influence on α-sialon phase formation in SPS. The influence of heating rate is similar for both compositions, and slow heating rate slightly encourages α-sialon formation. Lower amounts of liquid phase (in average) decrease the rate of α-sialon phase transformation, and this indicates the usual solid–liquid–solid mechanism. The application of higher heating rates seems to promote the formation of α-sialon with higher *x*-values. This may be connected with the better solubility of AlN and lower 21R-polytype formation during the fast heating.

4. Conclusions

(1) *Temperature determination*: It was experimentally verified that the sample is exposed to a temperature 140–180 °C higher, and 40–80 °C higher than what is measured by a pyrometer on the outer surface of the graphite die during a momentary overshoot and during isothermal holding, respectively.
(2) *The role of the electrical current*: Electrical current and conductive connection does not seem to play a principal role in enhancing the formation of electrically not conductive α-sialon.
(3) *The role of the mechanical pressure*: The formation of α-sialon under SPS conditions is neither strongly dependent on mechanical pressure nor densification. The fact that formation of α-sialon can be completed before the full densification under SPS free sintering conditions opens up new possibilities for tailoring microstructure through kinetic engineering.
(4) *The role of the heat transfer*: High heat transfer efficiency from the heating source to the sample plays the principal role in enhancing the formation of α-sialon, and the influence of heat transfer is much stronger than that of heating rate.
(5) *The α/β-Si_3N_4 phase ratio of the starting powder*: The phase solubility of the precursor powders is still an essential parameter in determining the speed of α-sialon formation and grain growth under SPS conditions.

Acknowledgements

This work was supported by the Swedish Research Council (through grant No. 621-2005-6290) and the Slovak Grant Agency VEGA (through grant No. 2/4072/04) and APVV (through grant No. APVT-51-049702). We thank Professor M. Nygren for valuable discussions.

References

1. Omori, M., Sintering, consolidation, reaction and crystal growth by the spark plasma system (SPS). *J. Mater. Eng.*, 2000, **A287**, 183–188.
2. Mishra, R. S., Risbud, S. H. and Mukherjee, A. K., Influence of initial crystal structure and electrical pulsing on densification of nanocrystalline alumina powder. *J. Mater. Res.*, 1998, **13**, 86–89.
3. Shen, Z., Johnsson, M., Zhao, Z. and Nygren, M., Spark plasma sintering of alumina. *J. Am. Ceram. Soc.*, 2002, **85**, 1921–1927.
4. Peng, H., *Spark plasma sintering of Si_3N_4-based ceramics—sintering mechanism-tailoring microstructure-evaluating properties*. Doctorial Dissertation, Stockholm, 2004.
5. Shen, Z. and Nygren, M., Microstructural prototyping of ceramics by kinetic engineering: applications of spark plasma sintering. *Chem. Rec.*, 2005, **5**, 173–184.
6. Werner, P.-E., A Fortran program for least-squares refinement of crystal structure cell dimensions. *Ark. Kemi*, 1969, **31**, 513–516.
7. Anselmi-Tamburini, U., Gennari, S., Garay, J. E. and Munir, Z. A., Fundamental investigations on the spark plasma sintering/synthesis process II. Modeling of current and temperature distributions. *Mater. Sci. Eng., A*, 2005, **394**, 139–148.
8. Diaz, A. and Hampshire, S., Crystallisation of M-SiAlON glasses to I_w-phase glass-ceramics: preparation and characterisation. *J. Mater. Sci.*, 2002, **37**, 723–730.
9. Shen, Z. and Nygren, M., Kinetic aspects of superfast consolidation of silicon nitride based ceramics by spark plasma sintering. *J. Mater. Chem.*, 2001, **11**, 204–207.
10. Kizler, P., Kleebe, H. J., Aldinger, F. and Rühle, M., Extended X-ray absorption fine structure (EXAFS) study of secondary phases in Yb_2O_3-doped Si_3N_4 ceramics. *J. Mater. Sci.*, 1997, **32**, 369–374.
11. Rosenflanz, A. and Chen, I.-W., Kinetics of phase transformations in SiAlON ceramics: I. Effects of cation size, composition and temperature. *J. Eur. Ceram. Soc.*, 1999, **19**, 2325–2335.
12. Camuscu, N., Thomson, D. P. and Mandal, H., Effect of starting composition, type of rare earth sintering additive and amount of liquid phase on α↔β SiAlON transformation. *J. Eur. Ceram. Soc.*, 1997, **17**, 599–613.